

An Extended Bilayer Model for Domain Growth in Antiferroelectric Liquid Crystal Display

CHUL GYU JHUN,¹ KEN CHEN,² TAE-HOON YOON,³
JAE CHANG KIM,³ SEUNGJUN YI,⁴ AND
SUNG SIK SHIN⁵

¹School of Display Engineering, Hoseo University, Asan, Chungnam, Korea

²College of Information Science and Engineering, Ningbo University, Busan, Korea

³Department of Electronics Engineering, Pusan National University, Busan, Korea

⁴Department of Semiconductor and Display Engineering, Hoseo University, Asan, Chungnam, Korea

⁵School of Advanced Display Engineering, Hoseo University, Asan, Chungnam, Korea

We have investigated the domain growth of antiferroelectric liquid crystal display under the switching process by means of CCD camera pictures. Its dynamic behavior was simulated by our extended bilayer model. In this model, we supplement free energy of antiferroelectric liquid crystal display with the coupling coefficient between adjacent molecules in the same layer, because domain growth propagates parallel to the smectic layer. The mechanism of the domain growth in antiferroelectric liquid crystal display can be described by the extended bilayer model.

Keywords Antiferroelectric liquid crystal display; domain growth; extended bilayer model

Introduction

The discovery of antiferroelectric liquid crystals (AFLCs) has attracted researchers' attention from both fundamental and practical viewpoints, and significant research has been carried out to understand their characteristics [1–15]. The response time of AFLCs is several hundred microseconds due to the spontaneous polarization. This high-speed characteristic is suitable for displaying dynamic imagery since it is essential to avoid motion artifacts such as decreased dynamic contrast ratio, stroboscopic motion, and blurred moving edges [16]. The intensive research of surface-stabilized

Address correspondence to Chul Gyu Jhun, School of Display Engineering, Hoseo University, Asan, Chungnam 336-795, Korea. Tel.: 82-41-540-5899; Fax: 82-41-548-0650; E-mail: cgjhun@hoseo.edu

antiferroelectric liquid crystal display (AFLCD) has been carried out to understand their characteristics. Also there have been many efforts to simulate dynamic behavior of AFLC cell [10–12]. These are only focused on hysteric characteristics of AFLC cells or thresholdless switching of frustrated AFLC cells, not focused on domain growth in AFLC cells.

In this work, we have investigated the domain growth of AFLCD under the switching process by means of CCD camera pictures. From our experiments, the domain growth of AFLC cells [13,14] is analyzed by the extended bilayer model. When driving pulses that consist of a selection voltage, a bias voltage, and a reset voltage [15] are applied to the AFLCD, the dynamic behavior is simulated.

Domain Growth in AFLCD

The test cells filled with AFLC mixture with the S_{CA}^* phase at room temperature are prepared. The thickness of the cell gap was $1.4\text{ }\mu\text{m}$. The sample is held in a hot stage (Mettler FP82HP) attached to a programmable temperature controller (Mettler FP90). The hot stage was fixed on the rotating stage of a polarizing microscope (Nikon Co.). Waveforms applied to the test cell were designed on a personal computer and sent via GPIB to a synthesized function generator (FLC, WFG500). Waveform employed in the experiments was SBR-AC. Addressing waveform with optimized bias voltage was tested for gray scale generation at 30°C .

In the AFLC cell, the domain propagation was apparently observed during the switching process from ferro-state to antiferro-state or intermediate state, when bias or reset voltage was applied to the cell. The antiferro-state propagates from the edge of the pixels to the center as shown in Figure 1 [13,14]. Particularly in the passive driving device, the domain growth properties can increase optical transmittance or reflectance of AFLCD because domain growth effect sustains optical transmission under the bias voltage [15].

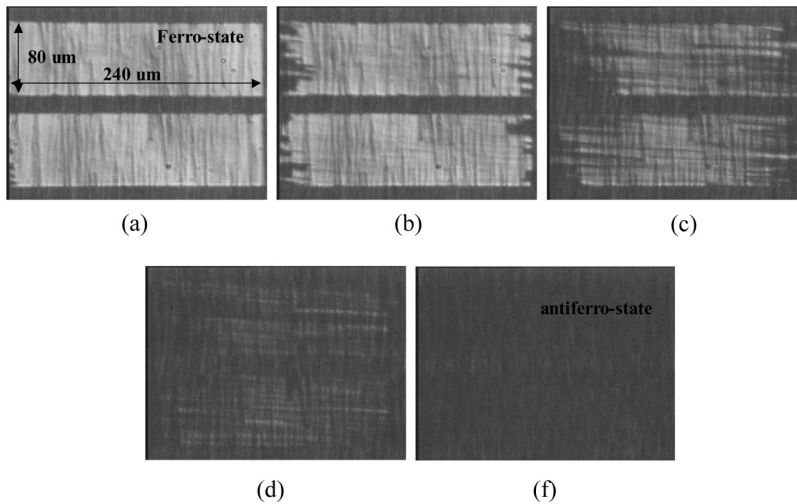


Figure 1. CCD images of domain growth, when AFLC cell is switched from ferro-state to antiferro-state: (a) Ferro-state; (b)–(d) intermediate state; and (e) antiferro-state.

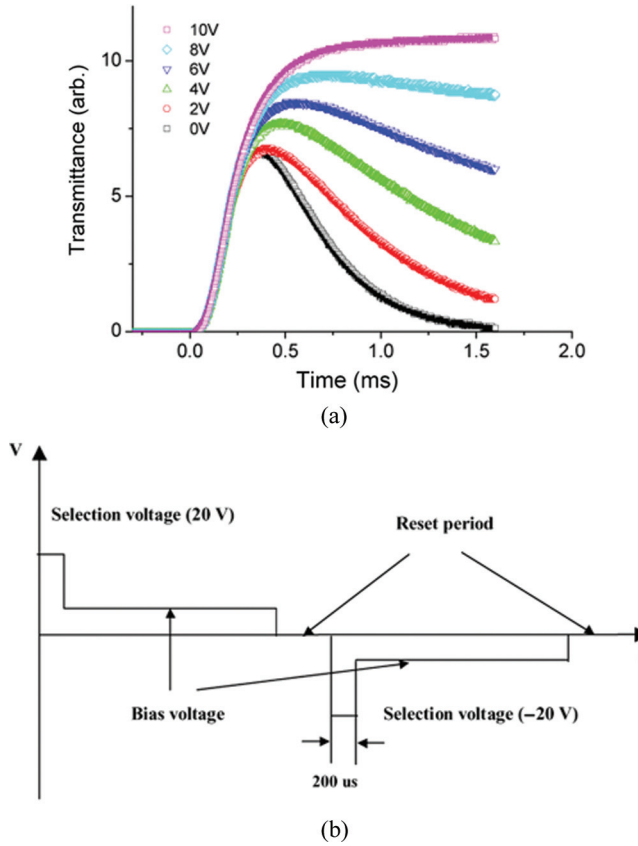


Figure 2. (a) Employed waveform (SBR) in the experiments and (b) optical response of AFLC cell with different bias voltages.

Figure 2 shows a delayed optical response with the variation of bias voltages, when driving pulses of SBR are applied to the AFLC cell. SBR pulses consist of a selection voltage, a bias voltage and a reset voltage. Pulse width and peak of the selection voltage are 20 V and 200 μ s, respectively. The optical responses were measured with different bias voltages at intervals of 2 V from 0 V to 10 V. The amplitude of the bias voltage has influence on the delay of maximum peak and steepness of optical response, because the propagating velocity of the domain growth is affected by the bias voltage [15]. Maximum brightness appears during the holding period. This effect is useful for high-resolution displays.

Extended Bilayer Model

Our model is based on the bilayer model. To simulate the domain growth in AFLCD, we assumed that each molecular in the same layer can separately rotate and considered the dipole interaction of each molecule in the same layer, since domain growth propagates parallel to the smectic layer [13,14]. Figure 3 shows extended bilayer model of AFLC, whose directors are in antiferro-state.

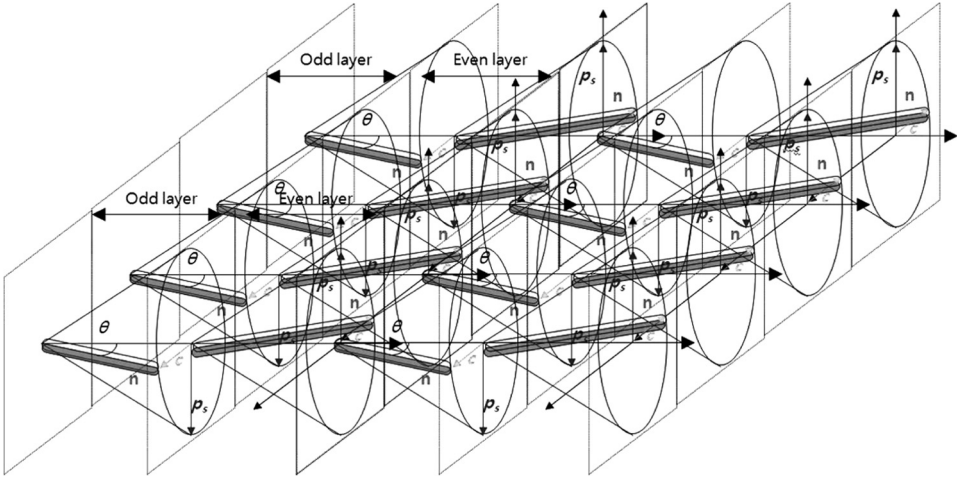


Figure 3. Extended bilayer model of AFLC in antiferro-state.

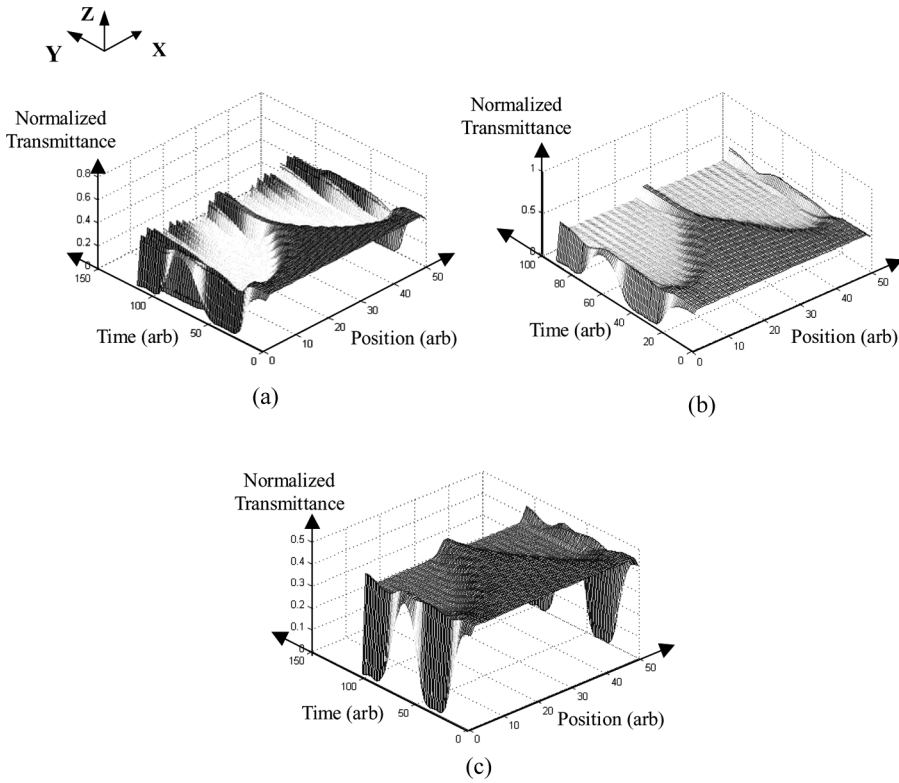


Figure 4. Simulation results of domain growth in AFLC cell according to bias voltages of (a) 0 V; (b) 2 V; and (c) 4 V.

Free energy of our model can be represented as:

$$\begin{aligned}
 F = & -\mu \sum_{i=-n}^{i=n} \mathbf{P}_{oi} \cdot \mathbf{e}_o - \mu \sum_{i=-n}^{i=n} \mathbf{P}_{ei} \cdot \mathbf{e}_e - K \sum_{i=-n}^{i=n} (\mathbf{P}_{oi} \cdot \mathbf{e}_o)^2 \\
 & - K \sum_{i=-n}^{i=n} (\mathbf{P}_{ei} \cdot \mathbf{e}_e)^2 - \sum_{i=-n}^{i=n} (\mathbf{P}_{oi} + \mathbf{P}_{ei}) \cdot \mathbf{E} + \gamma \sum_{i=-n}^{i=n} \mathbf{P}_{oi} \cdot \mathbf{P}_{ei} \\
 & - \gamma' \sum_{i=-n}^{i=n} \mathbf{P}_{oi} \cdot \mathbf{P}_{o(i+1)} - \gamma' \sum_{i=-n}^{i=n} \mathbf{P}_{ei} \cdot \mathbf{P}_{e(i+1)}, \quad (1)
 \end{aligned}$$

where \mathbf{P}_{oi} and \mathbf{P}_{ei} are the polarization vectors prescribed by the extended bilayer configuration. \mathbf{e}_o and \mathbf{e}_e are the fixed vectors in even and odd layers of cell boundaries, respectively [11]. μ and K are a polar and a nonpolar molecular field which is related to the surface anchoring effect. \mathbf{E} is the applied field. γ is the coupling coefficient between two polarization vectors in the adjacent even and odd layer. We supplement γ' term in free energy of AFLCD, which is the coupling coefficient between adjacent molecules in the same layer, because each molecule in the same layer should separately rotate.

Using the Landau-Ginzburg equations [11], the switching process from ferro-state to antiferro-state shown in Figure 2 was calculated. Figure 4 shows the simulation results of 1-dimensional domain growth in AFLC cell. The smectic layer in the AFLC cell is parallel to x-axis. X-axis represents the location of each molecule in the same layer; y-axis and z-axis represent time and transmittance, respectively. From the simulation results, domain growth propagates from the edge to the middle of the cell as time goes. When a higher bias voltage is applied to the AFLC cell, optical response has more delay time, because high bias voltage disturbs domain growth from ferro-state to antiferro-state under the bias voltage [15].

Conclusion

Domain growth of AFLCD was modeled with extended bilayer model, when driving pulses of SBR were applied to the AFLC cell. Its dynamic behavior was simulated by the extended bilayer model. In this model, we supplement free energy of AFLCD with the coupling coefficient between adjacent molecules in the same layer, because domain growth propagates parallel to the smectic layer. The mechanism of the domain growth in AFLCD can be described by the extended bilayer model.

Acknowledgments

This research was supported by the Academic Research fund of Hoseo University in 2009 (2009-0037).

References

- [1] Chandani, A. D. L., Hagiwara, T., Suzuki, Y., Ouchi, Y., Takezoe, H., & Fukuda, A. (1988). *Jpn. J. Appl. Phys. Part 2*, 27(5), L729.
- [2] Collings, P. J., et al. (1997). *Handbook of Liquid Crystal Research*, Oxford University Press, Inc.: United Kingdom, Chapter 5, 165.

- [3] Lagerwall, S. T. (1999). *Ferroelectric and Antiferroelectric Liquid Crystals*, Wiley-Vch: New York, Chapter 13, 325.
- [4] Johno, M., Itoh, K., Lee, J., Ouchi, Y., Takezoe, H., Fukuda, A., & Kitazume, T. (1990). *Jpn. J. Appl. Phys., Part 2*, 29, L107.
- [5] Beccherelli, R., & Elston, S. J. (1999). *Displays*, 20, 185.
- [6] Matkin, L. S., Gleeson, H. F., Baylis, L. J., Watson, S. J., Bowring, N., Seed, A., Hird, M., & Goodby, J. W. (2000). *Appl. Phys. Lett.*, 77, 340.
- [7] Judge, L. A., Beccherelli, R., & Elston, S. J. (2000). *J. Appl. Phys.*, 87(12), 8433.
- [8] D'havé, K., Rudquist, P., Lagerwall, S. T., Pauwels, H., Drzewinski, W., & Dabrowski, R. (2000). *Appl. Phys. Lett.*, 76, 3528.
- [9] Jhun, C. G., Kang, J. W., Yoon, T.-H., & Kim, J. C. (2003). *Opt. Eng.*, 42(7), 2047.
- [10] Nakagawa, M. (1991). *Jpn. J. Appl. Phys.*, 30, 1759.
- [11] Mottram, N. J., & Elston, S. J. (1999). *Liq. Cryst.*, 26, 1625.
- [12] Fournier, J., Pauwels, H., Zhang, H., & Becherelli, R. (1999). *SID'99 DIGEST*, 682.
- [13] Park, W. S., Jhun, C. G., Kang, J.-W., Choi, D. W., Han, K. Y., Yoon, T.-H., & Kim, J. C. (2002). *SID'02 DIGEST*, 480.
- [14] Quentel, S., Rodrigo, C., & Otón, J. M. (1996). *Journal of the SID*, 4, 19.
- [15] Jhun, C. G., Park, W. S., Kang, J. W., Yoon, T.-H., & Kim, J. C. (2004). *Mol. Cryst. Liq. Cryst.*, 410, 443.
- [16] Lee, B.-W., Sakong, D. S., & Chung, K. H. (2001). *SID '01 Information Display*, 17(12), 26.